International Journal of Engineering and Technical Research (IJETR)
ISSN: 2321-0869 (O) 2454-4698 (P), Volume-6, Issue-1, September 2016

Raman Spectroscopy, Review

Paul Rostron, Safa Gaber, Dina Gaber

***Abstract*— Raman spectroscopy is a branch of vibrational spectroscopy, which allows an easy interpretation and highly sensitive structural identification of trace amounts of chemicals based on their unique vibrational characteristics (fingerprints). Due to the continuous technical improvement in Raman spectroscopy, an advanced development of the device was achieved and more applications have become possible. This review is the first one to illustrate most of the main types of Raman spectroscopy in a single review. We present the general idea of theoretical and instrumental Raman device. The aim of this review is to highlight potential applications of different types, especially the application developed to identify corrosion products. It includes information about various types of corrosion product and a database presenting some corrosion products. This review ends with a concluding section summarize the main points of the review. Raman scattering is a spectroscopic tool predicted first theoretically by Smekal in 1923 and experimentally by Raman and Krishnan in 1928. Raman spectroscopy is vibrational technique involve high energy photons based on the inelastic scattering of radiation in the visible or near-infrared region of the sample. Most of the scattered light (Rayleigh scatter) has the same wavelength as laser source light. There are two types of light scattering the elastic and inelastic scattering. The elastic scattering is when the photon frequency doesn't shift or change its wavelength. The opposite is the inelastic scattering, which is involved in Raman spectroscopy. The shift of the frequency can be used to get an information about the molecular chemistry.**

***Index Terms*— Corrosion, corrosion detection, Raman spectroscopy.**

I. INTRODUCTION

Raman spectroscopy is a technique specialized in measuring the frequency shift of inelastic scattered light from the sample when the photon from incident light strikes a molecule and produce a scattered photon [1-5]. The out coming scattered light can be a photon with a lower frequency than the original photon and in that case, it is known as stokes Raman scattering or with higher frequency and known as anti-Stokes Raman scattering [6]. In the latter case, the photon will get energy from the bond of the molecule when the bond is initially in the excited vibrational state [7,8]. Generally, Raman is based on measuring the shift in the energy of the outgoing photon. The shift in wavelength of the scattered light depends upon the chemical composition of the molecules responsible for scattering. The intensity of Raman scattering is proportional to the magnitude of the change in the molecular polarization. According to Raman selection rule, the change in the molecular polarizability will be the result of the displacement of the constituent atoms from the equilibrium positions as the result of the molecular vibrations [9].

For many decades Raman spectroscopy had a limited application because of very low efficiency of the normal Raman scattering and the spectrometer parts were expensive and not suitable for on-site analysis [8]. Significant development and enhancement happened to Raman spectroscopy structure allow it to overcome those limitations and change the capabilities of the spectroscopy fundamentally where a portable and relatively cheap devices are now available [10]. Raman spectrum can be treated as a fingerprint tool for different compounds [8]. So the obtained spectrum of the analyte can be used as qualitative analysis for unknown samples or a mixture of components.

II. INSTRUMENT AND SPECTRUM

A Raman spectrometer is composed of light source, monochromator, sample holder and detector. Dispersive Raman spectroscopy and Fourier transform Raman spectroscopy (Fig.1) are different in their laser sources and by the method of detection for Raman scattering. Both techniques showed unique advantages and the method that best suit the sample should be preferred [11]. Several types of lasers can be used as the excitation source, like krypton ion (530.9 and 647.1 nm), He:Ne (632.8 nm), Nd:YAG (1064 nm and 532 nm) argon ion (488.0 and 514.5 nm), and diode laser (630 and 780 nm). Use of 1064 nm near-IR (NIR) excitation laser causes a lower fluorescent effect than visible wavelength lasers [12].

Raman spectroscopy has the great advantage of remote sensing when it is associated with optical fibers. The optical fibers are responsible to transport Raman signals by collecting the scattered photons. The fiber optic system includes fibers in which the laser excitation is transmitted along one fiber and the scattered radiations are transmitted to the detector along different fibers. Raman Spectroscopy has been used in real time monitoring system to detect illegal drugs, toxic material in the environment and chemical and biological warfare agents.

There is several commercially available hand held Raman spectrometers reviewed and mentioned by Ashley J., on 2013. Some of these spectrometers are, the SciAps ReporteRt (formerly DeltaNu, Inc.), the Snowy Range Instrument CBEXt, the Thermo Scientific FirstDefendert (formerly Ahura, Inc.) and the B&W TEK NanoRamt [13].

Paul Rostron, Department of Chemistry, The Petroleum Institute, Abu Dhabi, UAE, +97126075217.
Safa Gaber, Department of Chemistry, The Petroleum Institute, Abu Dhabi, UAE, +971501107167.
Dina Gaber, Department of Chemistry, The Petroleum Institute, Abu Dhabi, UAE, +971507200115.

III. RAMAN TYPES

A. Surface Enhanced Raman Spectroscopy (SERS)

Surface-enhanced Raman spectroscopy (SERS) is one of the most sensitive devices that allows for highly sensitive structural detection of low concentration analytes through

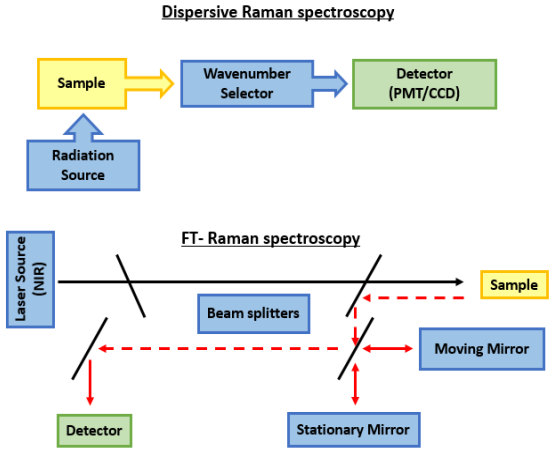

Fig. 1: Raman instrumentation.

the amplification of electromagnetic fields generated by the excitation of localized surface plasmons (LSP) of adsorbate molecules on the roughened metal surface [14]. The first published paper reporting the strong Raman signal from the interface was done in 1974 by Fleischmann and co-workers. The authors reported that the high intensity the signal is because of the large number of adsorption sites on the roughened surface [15]. Jeanmaire and van Duyne [9] and Albrecht and Creighton [4] groups in 1977, proved that the high intensity of Raman signal is due to the large increase of the Raman cross section of the adsorbed molecules which known as surface enhanced Raman spectroscopy. However, additional studies proved that SERS has resulted from a combination of two effects the electromagnetic effect and a resonance -like charge transfer effect [9].

While the signals obtained by normal Raman scattering is usually weak, SERS can detect very low concentration of the analytes because of the large increase of the Raman cross-section of an analyte up to 15 orders of magnitude in comparison to normal Raman scattering [8, 16]. Fig. 2 is a sketch that presents the main parts and component of Surface enhanced Raman scattering device [4].

Colloidal metals and roughened metal electrodes are SERS-active surfaces [17]. Colloidal metal is easy to be prepared and characterized because of its morphology and size. Even though it usually shows a relatively strong activity for the adsorbed molecules it has poor reproducibility of their properties because it is difficult to control its size [17]. The first recorded SERS spectra was by using a roughened silver electrode [18]. Another type of metal surfaces was tested after that like gold and copper. All those metal surfaces increased the intensity of Raman signal up to 104 to 106 fold. In general silver and gold substrate are the most often used types because they are the most air stable materials. Copper on the other hand is more reactive with air, which will affect the success of SERS [14]. SERS substrates become available in various shapes and coating after advance development. As an example, Shell isolated nanoparticle- enhanced Raman Spectroscopy [19]

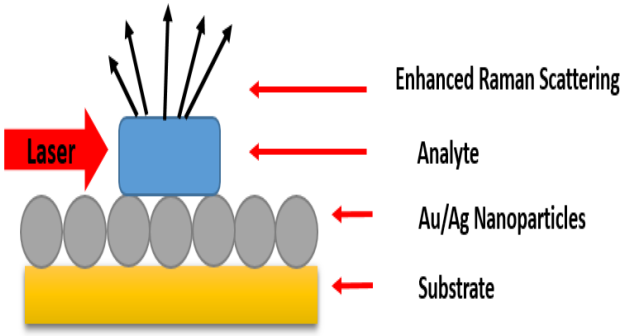

Fig. 2: Surface enhanced Raman scattering system.

and 2D Au nano-mushroom arrays [14]. The development in the metal substrate enables the technique to give faster and more accurate detection results for chemical and biological samples [16]. Different concepts have been developed to enhance the fabrication of SERS substrates using bottom up and top down approaches. The most important thing to realize to improve SERS is to provide the industry with more sensitive, cheaper components for the structure of the spectroscopy and simpler fabrication method. In this Perspective a brief review was published in 2014 by Jordan F. Betz describes some of the popular methods for SERS substrate fabrication and discuss the characteristics of simple SERS substrates [20]. Also other fabrication methods for SERS substrates have covered by many reviews papers [21–24].

The laser can be designed using gas, dye and solid state as excitation sources for analyte to produce Raman signal [9]. Choosing the best laser source will depend on the wavelength needed for the absorption band of SERS substrate and the power to avoid the formation of the interference [25]. Tunable lasers will be more suitable to match the excitation frequency of the substrate. The limitation is the complications of the process to prevent Rayleigh-scattered photons from reaching the detectors [9].

B. Surface enhanced hyper Raman Scattering (HR) scattering

Surface enhanced hyper Raman scattering is an inelastic sum of frequency scatted from two photons while the normal Raman scattering result from single photon. Total surface enhancement factors of SERS can be estimated to be the order of 1014. The enhancement can be the result of molecular electronic resonance where the molecular transition corresponds to the sum frequency of the incident photons [26]. A higher surface enhancement for hyper-Raman scattering can be achieved if both the surface effect and resonance effect are applied together [17]. Most of SEHRS experiments were done at 1064 nm excitation using mode-locked [27-29] Nd:YAG lasers or Q-switched [30,31]. Van Duyne group in 1988 [26], presented the first report of SEHRS spectra with experiment and theory for the vibrational assignments. Also, it was found that compressing the pulse to few picoseconds can increase SEHRS intensity.

SEHRS has also been tested for biologically relevant applications. An early study was performed by the Kneipp group where they used SEHRS to record the stretches of the bond of biological samples like amide I and III and C-O bond in the DNA [32]. Also SEHRS can be used to study the redox

reaction on electrode surfaces [33]. The research studies proved that SEHRS can be used as a potential ultrafast technique to study the dynamics of complex reaction with sensitivity higher than the one which can be acquired by SERS. In addition, SEHRS can be used to study excited states like what was demonstrated by the Camden group [26].

Appling the unique second-order non linearity multiphoton plasmonic enhancement and the intrinsic frequency doubling will give the advantage for SEHRS to be considered as a useful technique [34,35].

C. Tip enhanced Raman Spectroscopy (TERS)

Many research interest require Raman imaging of a small area within the sample, however conventional Raman technique can be misleading in some cases due to the masked signal contribution by the surrounding area signals [1]. Such issues encouraged further research on Raman scattering enhancement. Tip enhanced Raman spectroscopy (TERS) is one of the powerful solution that combines between two techniques; scanning probe microscopy and Raman spectroscopy [36]. TERS can provide a topographical and spectral/ chemical information simultaneously using SPM and Raman respectively [36,37].

TERS has similar instrumentation, material requirement and enhancement principle as SERS, but by using a metal tip or metal nanoparticle instead of the metal film [37,38]. The TERS technique is based on the fact that a metal tip or a metal nanoparticle is brought into close proximity of nanometer distance with the sample. An excitation laser beam will illuminate the tip apex creating an enhanced and confined electric field zone. This localized field will result in enhanced Raman scattered light from the sample located under the tip [39,40]. A diagram of TERS concept can be seen in Fig.3 [41]. The mechanism behind TERS ability to enhance the electromagnetic field at a tightly focused spot can be attributed to surface plasmon resonance and electrostatic lighting rod effect [40]. Further details were discussed in other sources [42].

There are three main scanning probe microscopy modes that are used in TERS experiments. The most commonly used is the Atomic Force Microscopy. The other two SPM modes are Shear-Force Microscopy and Scanning Tunneling Microscopy [37].

One of the most important requirement for the successful use of TERS is the optical alignments and geometry [37,43]. The illuminating laser should properly focus at the tip apex -sample interface while the scattered Raman should be collected efficiently. Several set-up configurations are available in recent years, reflecting the flexibility of TERS [18]. As can be seen in Fig.4, the tip can be illuminated in three ways; bottom or back reflection illumination, side illumination and top illumination [41]. The bottom illumination works for transparent or very thin film sample. While the other two are used also for opaque samples [43]. Each of these illumination techniques has its own limitations and advantages as discussed in the Gibson review [36]. The selection is mainly based on the analyzed sample and the SPM modes.

TERS can be divided into two techniques point scanning and mapping [36]. The latter is more efficient as it provides topographic and spectroscopic simultaneously. Most of

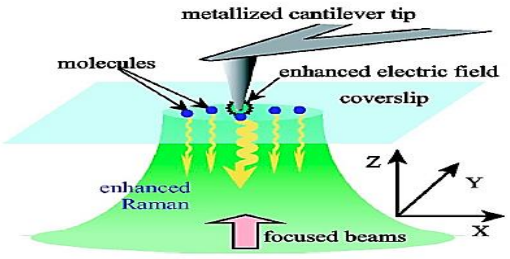

Fig. 3: Tip enhanced Raman spectroscopy concept.

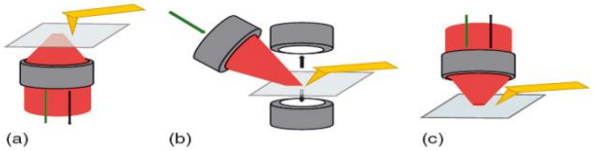

Fig. 4: Diagram alignmentferent optical alignments setup in TERS. (a) Bottom illumination (b) side illumination (c) bottom illumination.

research deals with point scanning, although it cannot provide a correlation between the chemical information about Raman data and the structural feature of the sample [44,45]. In some cases, line scanning can also be used especially when the sample consists of a multilayer [46].

The concept of TERS was first proposed in 1928 by Synge [47]. However, the concept was considered impractical until the second half of the twentieth century. In 1985, Wessel provided the theoretical concept of combing SERS enhancement and SPM resolution in TERS measurements [48]. As a result, TERS concept is mostly attributed to Wessel. Later on, at 2000 the experimental evidence was reported by Stöckle et al [39], Anderson [49] and by Kawata et al. [50].

Tips of TERS are fabricated using two noble metals either Au or Ag [37,51]. While Ag are preferred in term of higher field enhancements, Au are more stable. Ag are susceptible to degradation due to oxidation [37]. Current area of TERS research is working on identifying more reproducible and robust tips design and materials.

TERS is a great Raman tool that combines signal enhancement, high sensitivity with excellent spatial resolution of few nanometers [14,38]. TERS scattering enhancement has been reported to be in the range of 1010 to 1012 [1]. For instance, about 109 enhancements were obtained experimentally by Neacsu et al. [8]. The most important feature of TERS in comparison with SERS is the quantitative analysis possibility because of the identical electromagnetic field enhancement at all points [39]. In addition, TERS enhanced the reproducibility issue of SERS techniques [36]. Another advantage of TERS is its ability to work in the presence of water and humidity [37].

TERS is powerful tools in a wide range of fields. It was successfully applied in nano-structural investigation of both organic and non-organic materials [13]. For example, detection of single-walled carbon nanotubes was reported by using TERS [40]. Using such technique of high spectral resolution, it was possible to detect any fluctuation in the spectra due to SWCNT structural changes [52]. CNT are not the only carbon material investigated by TERS. TERS have been successful in providing information about the chemistry and structure of other carbon materials such as carbon nanotubes [53] and graphene [46,54].

Another area of interest in using TERS is bio-organic compound investigation, including nucleic acid, DNA and RNA identification [40,55]. Additionally, TERS are powerful tools in cell analysis, lipids and single virus particle [18,36,55]. TERS ability to give a spatial resolution of $1nm^2$, give it the possibility to analyze single biological molecules [37]. A reliable spectra of single RNA strand was reported using TERS [56]. It can be considered as a successful initial step toward a direct sequencing of single biomolecule. Another example, is the Raman spectra of shell components of a single bacteria as reported by Popp and coworkers [57]. Many ongoing researches are focusing on using TERS as a reliable and reproducible technique for biological samples. Extensive reviews on this topic and other applications such as catalysis and polymer blends are available in the literature [37,40,55]. Naresh Kumar has recently produced a nice review about TERS wide range applications and principle [55].

Some issues need to be addressed in TERS before it becomes a common robust technique. First, TERS measurement and practice are still complex and challenging in real life [8,36]. Therefore, only a limited number of TERS application can be found. Further work on Tip fabrication is required mainly in term of its stability and commercial availability. Currently tip metal coating such as gold and silver metal coating are easy to be worn off [37]. Also, the metal used are not stable and strong enough to withstand harsh conditions. Many ongoing research is focusing on finding new materials. For example, alloys are one of the promising material to increase the lifetime of tips [37]. Among the different ongoing research, improving TERS probe stability and reproducibility received the highest priority [58,59]. Also, a lot of TERS research is trying to study the sample at better controlled environments like using stainless steel chamber that can be filled with the desired gas or evacuated in case of vacuum condition [60].

D. Coherent anti-Stokes Raman Spectroscopy (CARS)

Coherent anti-stoke Raman scattering spectroscopy known as CARS is a nonlinear Raman technique that used to enhance the Raman signal [61]. As the name indicated, it uses coherent laser beams to generate a signal with frequency higher than the excitation frequency, therefore it is considered as anti-stoke frequency technique. The initial idea of CARS is contributed to P.D. Maker and R.W. Terhune who described it as a three wave mixing process [4]. However, the first CARS construction is assigned to Duncan et al in 1982 [62]. Later on, in 1999 CARS have witnessed a major improvement by replacing the visible dye laser source with near infrared laser beams [63].

The main principle of this technique is based on using multiple excitation laser sources [64]. It involves pump coherent monochromatic field at frequency of ωp, and stoke excitation field at frequency of ωS, overlapping spatially and temporally. When the incident light is focused on the sample at small focal volume and probed by a third laser beam, a strong anti-stoke Raman signal is created at blue shifted frequency away from fluorescence effects and in the face matching direction [4,61,65]. A strong signal is created with frequency of ωas = 2 ωp – ωS, when the difference in the frequency of the incident light, Δω = ωp – ωS, is tuned to the Raman active molecular vibration of the sample Ωvib [61]. Hence, CARS are able to provide information about the intrinsic vibrational bond of the sample with three dimensional resolutions. Since CARs is a four wave mixing process, the signal has a quadratic dependence on the incident radiation (nonlinear), unlike the spontaneous Raman signal which has a linear dependence on the incident field intensity [66]. Fig. 5 indicates the diagram of CARS energy levels [64].

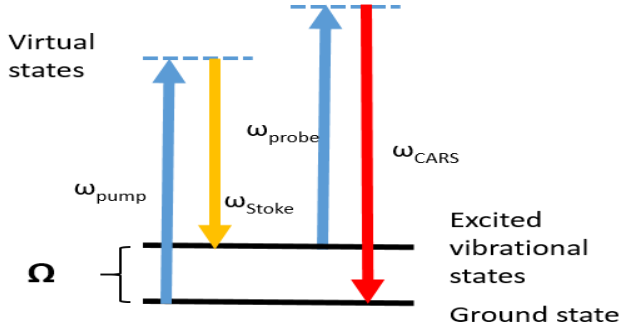

Fig. 5: Diagram of the coherent anti-Stokes Raman scattering (CARS) process [64].

The signal can be collected into two directions using two different geometries for excitation and detection. In the case of forward detected CARS (F-CARS) the signal is strong, but in some cases the signal can be masked by the non-resonant background signal from scatterers and solvent. Therefore, epi-detected CARS (E-CARS) are considered as a solution to overcome the non-resonant background from the solvent and improve overall sensitivity [62]. The E-CARS make imaging possible for new samples by introducing phase mismatching and detecting the signal in the background direction. Simultaneous use of E-CARS and F-CARS allow revealing various features in the studied sample. There are different other approaches to suppress the non-resonant background signal such as polarization coherent anti-Stokes Raman scattering (P-CARS) microscopy, frequency-modulation CARS and heterodyne CARS [66,67]. In 2009, a new approach was reported using a single-shot interferometric [68]. Time-resolved CARS microscopy (T-CARS) is another approach to improve signal to noise ratio based on using the Raman free induction decay of molecular vibrations [69]. Among the developments in CARS study, nanosecond, picosecond and femtosecond laser-based CARS techniques were used and reviewed extensively by many groups [67,70].

There are two types of CARS, single and multiplex frequency CARS [64,69]. While the first one concern individual vibrational resonance, the latter covers a broad range of vibrational resonance. As a result, multiplex CARS are slower, but provide more spectral information than single frequency CARS. Single frequency CARS record the response from each location of the sample at the specified frequency, therefore it is used in qualitative analysis to save time, while multiplex frequency is preferred in quantitative approaches [64]. With respect to the quantitative use of CARS. Several methods have been developed by researchers to gain quantitative information from CARS. These methods include experimental as well as mathematical approach, but generally can be classified into two groups, phase extraction and separation of the resonant and non-resonant responses. An extensive review and comparison of these methods advantages and limitations was provided by James and his group [64,71].

CARS is an anticipated alternative to spontaneous Raman spectroscopy. It offers high sensitivity, chemical specificity in addition to excellent spatial and spectral resolution [61,66,72]. Due to the coherent nature of Raman spectroscopy, a strong signal is generated with a sensitivity of around 5 orders of magnitude more than spontaneous Raman [63]. Accordingly, CARS require lower excitation power than conventional Raman and hence CARS can be noninvasive and tolerable by sensitive biological samples [4,73]. Another advantage is the fact that CARS can help in monitoring dynamic biological process due to the fast speed imaging that approach video rate speed. Conor L. Evans combined the CARS with video rate microscopy and investigated the possibility of in-vivo chemical imaging of lipid-rich tissue [74]. The results were promising as image were obtained at high speed and with high contrast. Moreover, the nonlinear excitation of CARS and the signal generated only at the focal spot gives CARS its intrinsic three dimensional sectioning capability [67]. Among the advantages, CARS signal is blue shifted which means that the signal will be insensitive to fluorescence interference [4,67]. Overall, due to the enormous properties of CARS which range from fast speed to depth penetration abilities, CARS are involved in many applications and research in recent years. CARS are receiving special attention from biological researchers due to its structural specificity and no labeling requirement [74,75]. It is used in many live cell or organism studies, including liver, skin and brain tissue imaging as well as lipid metabolism [73,76]. Also, it aids in understanding cancer classification and mechanisms [74]. Among the important biological use of CARS is studying drug delivery and distribution [75]. CARS does not only contribute to animal and human study, but also plants. CARS were used to study the distribution of lignin within the wall of individual cell of corn Stover [74]. A published review of the recent advances in linear and nonlinear Raman spectroscopy, reported the use of CARS in the measurements of temperatures and relative species concentrations in gas phase [70].

Although, CARS are mostly known to be used in biological and medical application, there are other fields where CARS have shown promising results such as material science [77], catalysis [78] and kinetic reactions [79]. In recently published review by Iwan W. Schie, some examples about the results of combining CARS with other techniques such as second harmonic generation (SHG) or two-photon excited fluorescence (TPEF) were reported [75]. It has been indicated that such combination can give further insight to the material under study.

There are still some drawbacks that should be solved. One of the main limitation is the non-zero background nature [77]. This is mainly due to the sample and solvent, electronic origins which contribute to the third order susceptibility, hence limiting CARS ideal sensitivity. Although studying dynamic system is possible by CARS, it is still affected by laser instabilities and signal fluctuations in the small time scale [67]. Similar to stimulated Raman spectroscopy, ongoing research is trying to simplify CARS in order to permit its commercialization in the near future [93]. Also, an active area of research is trying to extend the penetration depth mainly through adaptive optics [74].

E. Stimulated Raman Scattering (SRS)

SRS is another nonlinear process stands for simulated Raman Spectroscopy [80]. It was discovered by accident in 1962 when Woodbury and Ng observed an increase in radiation intensity without knowing its source [81]. Later on, Eckhardt attributed this increase to two photon process and simulated Raman scattering [82]. He proved that through his experiments. On the other hand, theoretical description was provided by Healthwarth [82]. A short time after this early discovery, a lot of experiments conducted and SRS was used in the analysis of atomic and molecular gases, liquids and solids [83]. The basic principle of this coherent phenomena is based on the incident of two photons (pump and stoke) like CARS principle [84]. The two laser beams coincide on the sample. When the frequency difference matches the molecular vibration frequency of a bond in the target molecule, this will induce simulated excitation in the vibrational transition. Consequently, this will result in stoke field amplification where the intensity of the stoke experiences a gain and pump- field attenuation where the pump intensity experiences a loss known as stimulated Raman gain (SRG) and stimulated Raman loss (SRL), respectively [84,85]. It should be mentioned that SRS are not identical to CARS. Although both are coherent phenomena that based on two incident photons. The SRS does not have a signal at frequencies other than the excitation wavelength [84]. Another difference is that SRS has a linear dependence on concentration and the resulting spectra match with spontaneous Raman spectroscopy, making interpretation much easier than CARS [85]. Also, the SRL and SRG only occur if the frequency difference matches a molecular resonance. As a result, unlike CARS, stimulated Raman spectroscopy does not have a non-resonant background (background-free) [86]. However, SRS signal is less intense than CARS signal [84].

Simulated Raman spectroscopy as a coherent Raman technique, allows an enhanced real time imaging, overcome the low signal intensity of spontaneous Raman spectroscopy and improve signal to noise ratio [83]. Additionally, the photon flux is directed collinearly with the probe laser, that means that SRS are not sensitive to the background fluorescence, since only a small fraction of this fluorescence is emitted collinearly with the probe [87].

SRS is an attractive imaging tool in the analysis of several vibrational bonds. This analysis has aided in the accurate determination of several bond lengths such as C-F bonds [88]. Its capability has been shown mostly in biological application such as distribution and uptake of drugs, lipid storage in living cells and skin tissue analysis [84-86]. As an example, quantification of lipid components such as cholesteryl ester and triacylglycerol has been demonstrated by Fu and co-worker using SRS imaging [89]. SRS has also been used in combination with multivariate curve resolution (MCR) to analyze and map a fatty liver tissue [85]. SRS can also be used in agrochemical and plant study. As an example, Mansfield et al. demonstrated the usefulness of using SRS in the analysis of the components of plant cell wall [90].

Continuous research and strategies aimed at enhancing SRS. For example, in the initial stage of SRS discovery. Narrow-bandwidth dye lasers were used to provide the probe. Later on, it was replaced by broadband Ti: sapphire lasers [87]. Among the developments, in 2007, the first femtosecond

stimulated Raman spectroscopy was reported by Ploetz et al [91]. Stimulated Raman spectroscopy has been discovered long time ago, however, their powerful potential in imaging has attracted a lot of recent research interests. Generally, most research is focused on improving pulse generation, involving SRS in more application and scaling down the complexity of the system. Several examples of recently published application of SRS can be found in the annual review of Laurence A. Nafie [92].

F. Resonance Raman Spectroscopy (RRS)

Resonance Raman spectroscopy is an instrument which measure the shift in the frequency of the photon when the energy of photons from the incident light is approximately similar to the energy needed for electronic transition [4]. The resonance excitation can increase the oscillation charge displacement of electrons. As a result, it will increase the induced dipole moment, which will directly enhance the efficiency of Raman scattering [6]. The enhancement factor of resonance Raman scattering comparing with normal Raman can be high as 108 [6]. It is important to note that fluorescence is more likely to interfere with resonance Raman more than non- resonance scattering.

Fluorescence is one of the challenges that limit the applicability of Raman technique. It was found that using UV resonance Raman spectroscopy for characterization of catalyst reactions and synthesis can eliminate the fluorescence effect. Most of the catalyst showed fluorescence spectra within the visible region so shifting the excitation laser to the UV region (λ <300 nm) will help to avoid interferences. Also, it can enhance the sensitivity of the technique to be used in many material sciences and biological fields [93,94].

Resonance Raman spectroscopy can be used to study the structure of hemi protein and the function of human body cell [95]. It can help to determine the shapes of potential surfaces or molecular geometries in excited states [96]. Also, it can be used for various analyses of biological samples like pigment and enzymes [4]. In addition, it can be used to study food protein structure [5]. In recent years, resonance Raman spectroscopy has been used as a technique to get vibrational spectra for specific sites in macromolecular systems [97].

G.Confocal Raman microscopy

The first confocal Raman microscopy was invented by Marvin Minsky in 1955 [98]. The probe head in Confocal Raman Microscopy work on focusing laser light on the sample through the microscope objective. And the pinhole will refocus the backscattered Raman signal which makes it behave as spatial filter. After that the signal will be collected on charge coupled device camera (detector) to produce a spectrum [4].

Depth profiling with confocal Raman microscopy can be applied in two ways. The first approach uses plotting of intensity of a specific band as a function of the distance from the sample surface. This way can provide information about the composition and structure of gradients of the sample. The second way is to acquire a pure spectrum of buried structures and used for identification determinations. [99].

Confocal Raman microscopy is known as “optical sectioning” and as non-invasive technique. It can provide an optical section of tissues without mechanical cutting or physical dissection. Many authors have used confocal Raman to study the layered system to obtain detailed information about the molecular composition. Also, it's been used for biological tissues because the optical sectioning avoids the need for any sample preparation and give high spatial resolution images [4,99].

In-situ chemical imaging of plant cell wall is possible using confocal imaging, also it can directly visualize the variation in cell wall polymer composition. In addition, the technique also enables detection of changes in orientation of the cellulose molecules. [100]. Confocal Raman microscopy has been found to be very effective to obtain information about the molecular composition in relation to skin architecture and can be used in different application of skin research [4]. Eugenii U. Donev team’s presented the first attempted to measure the structural changes of the nanoparticle vanadium dioxide with confocal Raman microscopy. Raman scattering could identify the lattice configuration and provide a direct way to obtain a statical information about the distribution of nucleation sites [101]. Raman confocal microscopy was used to identify and quantify glycation end product accumulation in ocular tissues. Tracking pathogenic can be useful to diagnose information about a range of diseases such as cataract formation and diabetic retinopathy [102].

Confocal microscopy is a useful technique to analyze local corrosion of metal and can be helpful in understanding corrosion mechanisms [103]. In general, this type of the Raman microscope has proven to be a useful analytical technique. It showed a set of advantages such as high spatial resolution, clear image quality in addition the sample need no preparation [98].

H.Raman imaging microscopy

Raman imaging is a technique found first in 1975 by Delhaye and Dhamelincourt [104] and it is capable to generate a detailed chemical image of the Raman spectrum [105]. In general, Raman imaging is a combination of Raman spectroscopy and digital imaging technique [105]. The direct Raman imaging is a function of Raman intensity and spatial coordinates and the color images are based on material molecular composition, phase, structure and crystalline [106].

As an example of serial imaging approaches are point and line Raman mapping. The difference between the two examples is the laser involve in scanning proses. Point imaging is involving a spot laser or a raster scanning in x and y dimensions and produce a spectrum with two spatial dimensions. In the line mapping approach, the laser line will scan either in x or y axis [106].

The technique is widely used in different application that cover a range of science, such as material science, medicine, polymer, artwork and semiconductors. It can be used to identify the drugs and toxic materials in forensic science and to analyze or understand the relationship between molecular structure of the sample and its functions in biomedical [106]. It was proven that an endoscopic Raman probe can demonstrate a good ability to provide a rapids and direct image based on Raman technique which can be used in clinical research and routine endoscopic inspection [107]. Furthermore, this technique can be used to study the drug distribution in living cells like cancer cells. [108,109]. Also Raman imaging can be used to study plants organs like seeds and leaves [110]. Raman imaging techniques can be classified to either direct or serial or what is known as raster imaging techniques. The direct imaging approach at a given wavenumber is where all spatial points in the Raman image

are determined simultaneously from a single measurement of globally illuminated sample. While, the raster imaging is where numerous spectra are recorded to construct the entire Raman image at specific wavenumber [106].

IV. RAMAN VS FT-IR

Raman and IR spectroscopy are similar but not identical techniques. It is true that both are types of vibrational spectroscopy, which deals with same vibrational energy levels of the material [111]. However, each one of these techniques is based on different ways of interacting with the studied object and the results are ruled by different principles. Generally, Raman scattering depends on the polarization change, while IR spectroscopy mainly depends on dipole moments change. Also, it was found that Raman spectroscopy can identify different components in sample mixtures much easier than IR spectroscopy due to Raman narrower bandwidth [112]. IR signal is produced upon IR light absorption. Since this technique uses long wavelength excitation, the corresponding spatial resolution is low [61]. The spatial resolution of IR was reported to be in the range of 2.5-25 μm [64]. Another issue with IR is related to water absorption [64,77]. The strong water absorption hinders IR use in bio-imaging, archeology and other studies that contain water or moisture in its studied structure. Such problems were avoided in Raman spectroscopy. This alternative technique can use an excitation laser source that works in the visible or near IR spectral range [64]. Also, Raman cross section scattering is lower than IR absorption. Consequently, Raman is not affected by the presence of air, water or glass and has a wider, extending applicability range [37,112].

V. CORROSION

According to DIN EN ISO 8044, corrosion is defined as: "Physical interaction between a metal and its environment which results in changes of the metal's properties and which may lead to significant functional impairment of the metal, the environment or the technical system of which they form a part." [113].

There are two types of corrosion reaction:

Electrochemical corrosion is the corrosion that includes reaction between anodic and cathodic parts. Chemical corrosion: reaction of the metal with environment, excluding electrochemical reactions.

Corrosion is a spontaneous and exothermic process can lead to wear and damage the structure of many industries [113]. The word corrosion is not specified for iron it is used for all materials and even some time nonmaterial things like the soul that wear out or damaged because of its instability toward a change of air component or flow of waters [114].

In 2013 it was reported that in oil and gas production industry the total annual cost of corrosion is estimated to be US$1, 372 billion divided as follows, around $589 million for pipeline and facilities costs, $463 million annually for downhole tubing costs, and $320 million for corrosion management and control costs [115]. In the oil and gas industry, it is important to use the most effective and sensitive detection, and control management methods to reduce the annual cost of corrosion. Corrosion not only affect the economics of the industries, but also it can affect the safety of the worker and the resident life, cause a health hazard by the release of some toxic compound from storage tanks which can also influence the environment [114]. Although the development in the industry lead to use multi-phase transportation of oil and gas, which increase the tendency for the risk of corrosion, many other factors can affect the severity and the type of the occurred corrosion [116].

Many factors can influence the corrosion layer formation, severity, and properties [114]. Corrosion is mainly affected by the air and water content or both of them. Also, many environmental parameters can influence the corrosion formation. Most of those parameters related to the chemistry of the water, the change of the temperature or pH, CO_2 partial pressure, pollution and the presence of H_2S, oxygen, and organic acids and the flow type and velocity. High CO_2 partial pressure, water chemistry and low pH can increase the severity of the corrosion [115].

A. Corrosion types

Corrosion can damage the material and cause a defect or fault in the industrial system. A simple representation in Fig. 6 explains the interaction and the definition of faults, defects and failures [117].

There are many types of corrosion which can happen to the metals. The following lines will explain each type of corrosion and method for prevention and control [117].

Uniform corrosion: The exposed parts of a metal surface to the acids, Aerated fresh water or salt water corrode uniformly leading to weakening the metal layers and then damage those parts. Industrial gases can increase the corrosion rate of the metal as an example of those gases Sulfur dioxide, Carbon dioxide and Nitrogen oxides [118].

Galvanic Corrosion: Galvanic type is a corrosion which occurs when two dissimilar metals are in contact and electrochemical series is formed. It requires the presence of electrolyte, metallic path in addition to the anodic and cathodic materials. The severity of this corrosion can be affected by the distance between the active and noble metal, temperature and the oxygen concentration. It's important to select the structural material and consider an inhibitor to consume cathodic depolarizers. Also, it will be better to avoid thread joints and build anodic materials to be easily replaceable to reduce the cost of the replacement process [113].

Pitting: is a corrosion that occurs when the protective film or the coasting of the materials break down. The exposed, tiny pits start to react with the environment and a localized corrosion form. The depth of the petting usually exceeds its diameter. [113]. The exposed metal gives up electrons easily, but the actual mechanisms of pitting are not clear. [115]. In general, the tendency of pitting can be affected by the temperature and carbon dioxide partial

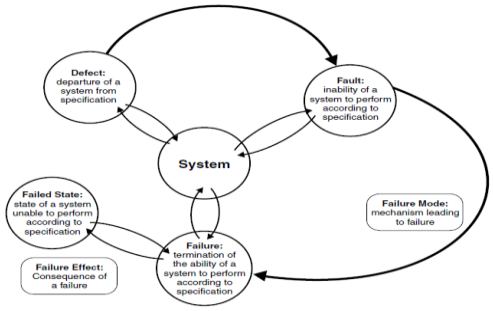

Fig. 6: Interrelation among defects, failures and faults Pressure [117].

Schmitt and coworkers studied the effects of temperature, Cl^- concentration, the nature of anions and cations on pitting corrosion. [116]. The severity of pitting corrosion can be control be selecting the best resistant material and controlling the chemistry of fluid [118].

Crevice corrosion: Crevice is a highly localized corrosion process start with an oxygen concentration reduction followed by a reduction in the pH of the system and an increase in the concentration of chloride ions. The process usually happened under the deposits, in the voids or gaps between metals and in the dead ends which make it difficult to be noticed or detected. Corrosion occurs rapidly and lead to the breakdown of the passive film as a result of high oxygen demand. To prevent crevice corrosion or reduce it using welds instead of bolts is required. Also, avoiding sharp corners and using sealant and blast resistant materials can help in the controlling process [118].

De-alloying: This is the type of corrosion which affect the alloy materials when the combination of its component have a large difference in its activity. It depends on flow rate and the concentration of oxygen. The problem with detection this type of corrosion is that it doesn't change the metal appearance, may be it will result in small differences in the volume, but if a cross section from the alloy is studied it will reveal the change in its color [118].

Environmental Cracking:

Hydrogen damage: (Hydrogen-Induced Cracking (HIC) and Hydrogen Embrittlement (HE)): Hydrogen can damage metal by different mechanisms. Hydrogen ion adsorbs onto the metal and then form a neutral hydrogen atom which combine with H radical and form hydrogen gas (H_2). The small size hydrogen ions and gas particle will migrate to defect parts and damage metal, cause blistering or cracks in the presence of tensile stresses, especially in the high hardness area of the metal [113]. As a result of hydrogen induced cracking and damage a sudden loss in the strength of the structure will happen. To avoid or reduce this type of corrosion it's important to use hydrogen free material or remove hydrogen in the metal by backing [118].

(H_2S) Sulfide Stress Corrosion Cracking: It was found that the presence of hydrogen sulfide (H_2S) can be one of the reasons to initiate the corrosion process specially in oil and gas industry. The formation of hydrogen sulfide can be by product of the industrial process or from microbial action. [115]. H_2S reacts with Iron to form Iron Sulfides and Hydrogen.

CO_2 Corrosion: sweet corrosion is the most dominant form of corrosion that face the oil and gas industry [115]. The first case of sweet corrosion was recorded in U.S. oil and gas industry in 1940s in gas wells located in Texas. [116]. The mechanism of CO_2 corrosion is complex and need further work [116]. In general, dry CO_2 is noncorrosive to steels and alloys so first CO_2 dissolve in water to promote an electrochemical reaction and form carbonic acid [115, 116]. Iron carbonate can be formed on the steel surface and then when it precipitates it can act as a protective layer. The protective layer can be destroyed as a result of environmental condition and the presence of H2S and a localized corrosion can take place as (1) (2) and (3). [116]

$$Fe^{2+} + CO_3^{2-} \leftrightarrow FeCO_3 \quad (1)$$

$$Fe^{2+} + 2CO_3\ H^- \leftrightarrow Fe\ (CO_3H)_2 \quad (2)$$

$$Fe\ (CO_3H)_2 \leftrightarrow FeCO_3 + CO_2 + H_2O \quad (3)$$

Sweet corrosion is affected by many environmental parameters. Chemistry of the water, pH of solution, temperature [115], CO_2 partial pressure and presence of H_2S [119] and the chemistry of metal of alloy [115]. Situ pH — pH of the solution can influence the precipitation and dissolution of iron and effect the corrosion rates [116]. The effect of H_2S — H_2S can either increase rate of CO_2 corrosion by affecting the pH or decrease it by forming sulfide scale as a protective layer. The presence of organic acids influences the sweet corrosion because it reduces the protectiveness of the films. In addition to environmental parameter, several physical parameters can affect the rate and the severity of CO_2 Corrosion. Theses physical parameter includes wax [116], crude oil [120] and fluid dynamics which is part of the oil and gas industry [116].

Microbial Corrosion: is the degradation of materials as the result of the presence of fungi, molds and bacteria or their by-products. It can attack the material itself of the coating layers by acid by-products, sulfur, hydrogen sulfide or ammonia [118].

B. Corrosion detection methods

Predication models are developed for oil and gas industry to predict CO_2 corrosion in its pipelines. These models are either based on empirical correlations with laboratory results of field data or based on mechanistic modeling of different process of CO_2 corrosion. The main problem with those predication models is that it can predict low corrosion rate while the actual situation is very high in the field. Also, it can give false information that the corrosion rate is very high while it is not the case and affect the production process [121]. The corrosion inspection and monitoring is very important to give accurate information about the situation. Non- destructive evaluation techniques are the most favorable method for industry to get critical information about the system. Many inspection techniques were used for corrosion evaluation like the visual inspection, electromagnetic, thermographic inspection and ultrasonic system. [117].

Visual inspection requires human staff to enter the pipeline looking for evidence of corrosion [122]. Ultrasound evaluation is done using a beam of sound waves. The sound wave is reflected as a result of the change of the density of the material. One of the limitation of this technique, it requires an accesses and complete cleaning of the pipe before inspection [122]. Some industries usually run the inspection for corrosion using CCTV (closed-circuit TV) cameras. The technique is lacking the visibility in the interior of pipes and the image is poor in quality because of the difficult lighting conditions inside the pipes [123]. A physical sensor based on reflectance theory and experimental data is more accurate than CCTV. The sensor intensity can be extracted to give a map image for the internal side of the pipe in addition to the ability to sense the defect parts [123]. Now a days using Raman Technology for corrosion inspection can save time and money for oil and gas industry.

VI. APPLICATION OF RAMAN IN CORROSION

Numerous techniques have been employed to measure and study the corrosion of the steel surface like X-ray Photoelectron spectroscopy (XPS) [124], secondary ion mass spectrometry (SIMS) [125], atomic force microscopy [126],

and Raman spectroscopy [127]. Most of the available corrosion detection techniques require extensive sample preparation methods, it also can't be used in aqueous condition [128]. This is the advantage of using Raman spectroscopy for the characterization of corrosion where no extensive sample preparation is needed and it can be employed under aqueous conditions. Raman spectroscopy also offers the advantage of identifying hydrogen bonds, which is difficult with standard characterization methods such as XPS (X-Ray photoelectron spectroscopy) [128]. Generally, Raman spectroscopy is widely used in unknown identification and characterization because it depends on the intrinsic vibrational modes in the studied material. Therefore, Raman is considered as an extraordinary finger printing tool that provides a large number of information applicable for condensed, gas phase and even non-crystalline metals [112,129].

A nice example of Raman efficiency in corrosion study was done by De Faria et al [130]. The corrosion products of steel were identified using a Raman spectrometer with laser light at 532nm and at low powers from 0.025 to 0.25mw and laser light at 633nm at higher power between 2.5 and 25 Mw. The corrosion products found to be iron oxy hydroxides, goethite and lepidocrocite. Also, it was found that some corrosion product will give higher and sharper peaks when the laser powers increased to 0.25 and 0.5 mW such as goethite [130].

Many studies have indicated that corrosion products are usually composed of several iron oxide layers [131-135]. Among corrosion products discussed previously, rust products in carbon and weathering steel have received a wide attention due to their widespread and severe effects on pipeline, instruments and ancient artifact lifetime. Rust forms thick layers over time and its composition can differ depending on the environment condition such as atmospheric, aerated or anoxic soils surroundings [136]. Also, the type of materials and other factors like the presence of chloride ions, pH and temperature can lead to different compositions [137]. For example, Xin Zhang identified the outer layers which is in contact with the environment is composed of lepidocrocite (ɤ-FeOOH), while goethite (α-FeOOH) or magnetite (Fe_3O_4) can form in the inner parts according to the corrosion conditions [11]. On the other hand, a study by Xianhai Nie has indicated α-FeOOH formation in the inner layer of carbon steel, while the outer layer consists mainly of Fe_2O_3 and Fe_3O_4 under salty soil environmental [138]. Generally, it is believed that α-FeOOH is the initial corrosion product in steel which can transfer to other form according to the conditions [138].

Here will focus on some literature studies on iron corrosion, including different oxides and hydroxides using Raman spectroscopy techniques. A nice recent study by Ludovic Bellot- Gurlet has reported the investigation of iron corrosion products under different environments [136]. In addition, a quantitative phase proportion was studied as can be seen in Fig. 7. Similarly, in 2015 Toshiaki Ohtsuka monitored the rust layer formation on weathering steels under alternating environment of wet and dry conditions for a long time (144 hours) and under the presence of sodium chloride deposits to represent the coastal environment [139]. Initially, lepidocrocite and magnetite were identified. Later on, other phases were identified, such as akaganeite in the presence of NaCl, which is known to reduce the rust protection property. Several groups have performed research on the effect of different conditions. As an example Xin Zhang studied the corrosion products formed in the presence of chlorine and sulfate [11]. Earlier studies by Reguer and coworkers [140] investigated the Chloride containing corrosion products. Nie and coworkers [138] worked on the corrosion of carbon steel in seashore saltysoils with different water content. Earlier study by S. Savoye et al. Reported the nature of corrosion products formed in the presence of carbonate and oxygen using Raman spectroscopy [137].

Delphin Neff with co-workers have devoted a lot of their research work to the analysis of corrosion products using Raman spectroscopy [132,141-143]. Most of their studies were performed on archaeological iron artifact samples. An interesting work published by Judith Monneir from the same group [144]. The work introduced a technique for extracting quantitative parameters from the Raman hyperspectral map using LADIR-CAT software. This approach was established specifically for the iron corrosion study. The results obtained from De Faria et al. [145] investigation showed that increasing the laser power can cause a change in the corrosion spectra were a hematite characteristic bands show up in the spectra of the most of

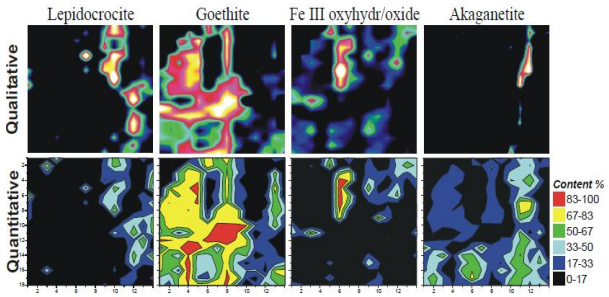

Fig. 7: Raman imaging results indicating a comparison between qualitative and semi-quantitative results from spectral decomposition

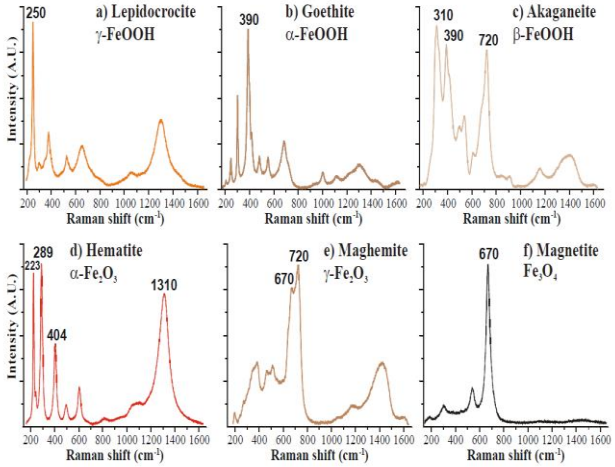

Fig. 8: Raman spectra of some iron corrosion products obtained at 532 nm and power <100 µW

the oxides and oxyhydroxides studied in his work. The laser power is a very important parameter which affects the obtained spectrum significantly. El Mendili et al. [146] found that the vibration modes attributed to the hematite become stronger with increasing the laser power and the thermal treatment. Singh et al [147] on the other hand, found that the noise in the Raman spectrum increased when the laser power become less than 1.5m W. It is important to differentiate if

hematite peaks produced from laser irradiation transformation or is it a component of corrosion products.

Several other papers have been reported on the investigation of different iron oxides with Raman spectroscopy and provide a large number of spectra that can be used as reference material [148-152]. An example of representative Raman spectra of the most common phases of iron corrosion products can be seen in Fig. 8 [136].

Unlike pure iron, very little investigation has been done on the characterization and identification of corrosion products in other materials such as AISI-4340 steel or Tin [128]. P. Eckold et al [153] used confocal "Horiba Lab ARAMIS" Raman microscope to detect $Sn_3O_2(OH)_{2-x}Cl_x$ phases as intermediates in tin corrosion. The Raman spectra were processed using Origin 8.0 and Lab Spec version 5.25.15 software.

The developed corrosion cell is consisting of a glass chamber equipped with specimen holder and sapphire window and then implemented within the Raman Spectrometer. Ashley C. Stowe [154] showed that Raman spectroscopy is an effective complementary method to detect lithium hydride corrosion since Li_2O vibrations are Raman active. Also found that using UV laser wavelengths to excite the sample will solve the fluorescence interferences while allowing all of the spectral features from LiH, LiOH, and Li_2O to be observed. Thiago S. Puglieri and his coworker [155] investigated the effect of relative humidity (RH) and formaldehyde (H_2CO) concentration on Pb corrosion. Raman images for the study were obtained using laser line from He-Ne and diode laser respectively, and the laser power was below 1.5 mW to avoid degradation [155]. In situ Raman spectroscopy was also used to study the hydrothermal corrosion of a zirconium- niobium alloy at temperatures ranging from 22 to 407^0C [156]. Spectra of the synthesized uranium compounds U (VI) were recorded to make the Raman spectral library to use it to investigate the unidentified materials on the corroded samples [157]. Copper corrosion was studied by R. L. Frost [158]. He reported and identified the different copper minerals identified by their characteristic Raman spectra. Other corrosion products were studied by other groups such as Mg, Zn and Cr oxides as indicated in Table 1 [159].

VII. RAMAN DATABASE

Raman identification is based on comparing the unknown spectra, which is characteristic to the material structure and bonds, with reference known materials [112]. As a result, the availability of such references is important to facilitate the analysis of materials. In addition, it offers a quicker way to identify the material and hence extend the use of Raman techniques in a wide range of application. The need for establishing a spectral database for different material inspired the work of many research groups [160-163].

Beside the different publications, nowadays there are digital, searchable libraries that offer an easy access to a wide range of materials including pigments, resin and minerals [164]. For example, RRUFF project website (http://rruff.info/) offers a wide range of good quality spectra of different minerals. Handbook of Minerals Raman Spectra (http://www.ens-lyon.fr/LST/Raman/index.php), is another nice online, spectral database, but have limited number of spectra. Romanian Database of Raman Spectroscopy-website (http://rdrs.uaic.ro/minerals/hematite.html) is another extensive source for a large mineral and pigments database. The site not only offer Raman spectra, but also give information about the crystal structure and sample image. The other interesting database is reviewed by Peter Vandenabeele and his team [164]. Another method for comparing spectral database are provided by HORIBA Scientific. It offers an extensive database searching package covering over 1500 spectra in different materials not only minerals. It is provided with advance features allowing correlation between the spectral peaks and the expected responsible functional group [165].

Table 1: Raman fingerprint of main corrosion products [159]

Compound	**Formula**	**Characteristic wavenumber**
Wustite	FeO	655
Hematite	Fe_2O_3/ corundum	1320,290,220
Magnetite	Fe_3O_4/ spinel	670
Maghemite	ɤFe_2O_{3x} H_6/spinel	670-720,~1400
Ferrihydrite	Fe_5HO_8, $9H_2O$	710-~1380
Goethite	αFeOOH	390
Lepidocrocite	ɤFeOOH	250-1300
Akaganeite	β FeOOH (Cl)	310,390,720
Ferooxyhyte	ɤFeOH	680,~1350
Hydroxychloride	β Fe_2 $(OH)_3Cl$	160,423
Green rust		430-510
Iron chloride	$FeCl_2$	610
Zinc chloride	$ZnCl_2$	80,248
Zinc Oxide	ZnO	100,540-580
Zinc hydroxide	$Zn(OH)_2$	470
Zinc carbonate	$ZnCO_3$	1095,370
White rust	$3Zn(OH)_2$ $2ZnCO_3$	1050,385
White rust	$4Zn(OH)_2$ $ZnCl_2$ $(OH)_4$. H_2O	910,3455-3486
White rust	Zn $(OH)_4$ Cl_2SO_4·$5H_2O$	955,208,292
White rust	$ZnSO_4$·$3Zn(OH)_2$. $3H_2O$	961,1007,463
Zinc phosphate	$ZnPO_4$	996
Zinc phosphate	$Zn_3(PO_4)_2H_2O$	1055,1150
Manganese oxide	MnO_2	~600
Nickel oxide	NiO	~510
Chromium oxide	Cr_2O_3	351,551,609
Chromium hydroxide	CrOOH (Cr_2O_3, n H_2O)	485
Machinawite	FeS	~280-300
Greigite	Fe_3S_4	~350-360

Although, noteworthy improvements have been made in the construction of the database reference library. Further work is needed to unify and provide a full spectra database that allow comparisons between the results obtained in different laboratories. It should be noted Raman spectra comparison can be tricky and should be handled carefully. Difference in laser source wavelength, crystal orientation, different calibration method can lead to some difference between the compared spectra. In addition, the different data reporting method can lead to apparent spectral differences [136,164].

VIII. CONCLUSION

Raman spectroscopy is a well-known powerful analytical tool that become increasingly important in recent years. The main

aim of this review is to present a comprehensive yet simple overview of Raman spectroscopy. After discussing the main Raman principle, instrumentation as well as its history and theoretical background. The various advanced Raman techniques have been presented such as surface enhanced Raman scattering (SRS), Coherent anti-stoke Raman scattering (CARS), Tip enhanced Raman scattering (TERS), stimulated and resonance Raman spectroscopy. We have shown that all these techniques aid Raman spectroscopy in overcoming its limitation through different approaches. In addition to enhancing the obtained signal, the Three sectioning capability and free chemical imaging become possible by CARS. Using TERS, quantitative approach and spatial resolution down to the Nano-scale was introduced through sub-diffraction imaging. SERS improved Raman sensitivity by several orders of magnitude involving a substrate material. Many other properties such as reproducibility and selectivity has been improved through the different techniques opening new application opportunities for Raman spectroscopy. The basic, advantages and limitations of each type of Raman subsets were highlighted. Nice examples on the applications of each type have been given. The wide range of application field ranging from biology and medical application to forensic and archeology, demonstrated the great potential of Raman technique that will continually increase in the future. Raman imaging and confocal Raman spectroscopy has been also discussed. In this work, we focused in the second part of this review on providing a detailed investigation highlighting the importance and the state of the art of Raman application in corrosion study. After a brief summary about corrosion type, causes and effects. We demonstrated a lot of great publications related to Raman spectroscopy and corrosion. However, we found that most of these works are based on spontaneous Raman spectroscopy. We believe that further involvement of advance Raman techniques in corrosion study can provide a great contribution to corrosion field study. Especially, with the latest developments of charge-coupled device (CCD) chips, filter technologies and analysis software which makes portable Raman instruments and even real time video possible. Generally, from this review, it is clear that despite the fact that all these techniques can still have some limitations, especially in regard to the system complexity and fluorescence interferences, the continuous research interest in Raman techniques can ensure its successful improvements and importance in the near future.

ACKNOWLEDGEMENTS

This work was supported by Abu Dhabi National Oil Company (ADNOC) Gas Sub Committee (GSC), Abu Dhabi, UAE project Number 14703 with the work carried out at the Petroleum Institute, Abu Dhabi, UAE. The authors thank the GSC for their support. We also appreciate Nannan Li's assistance with the manuscript.

REFERENCES

[1]Long, D. A. (1977). Raman spectroscopy. New York, 1-12.
[2]Raman, C. V., Krishnan, K. S. (1928). Polarisation of scattered light-quanta. Nature, 122, 169.
[3]Efremov, E. V., Ariese, F., Gooijer, C. (2008). Achievements in resonance Raman spectroscopy: Review of a technique with a distinct analytical chemistry potential. analytica chimica acta, 606(2), 119-134.
[4]Das, R. S., Agrawal, Y. K. (2011). Raman spectroscopy: recent advancements, techniques and applications. Vibrational Spectroscopy, 57(2), 163-176.
[5]Li-Chan, E. C. Y. (1996). The applications of Raman spectroscopy in food science. Trends in Food Science & Technology, 7(11), 361-370.
[6]Asher, S. A. (1993). UV resonance Raman spectroscopy for analytical, physical, and biophysical chemistry. Analytical chemistry, 65(4), 201A-210A.
[7]Kudelski, A. (2009). Raman spectroscopy of surfaces. Surface Science, 603(10), 1328-1334.
[8]Kudelski, A. (2008). Analytical applications of Raman spectroscopy. Talanta, 76(1), 1-8.
[9]Haynes, C. L., McFarland, A. D., Duyne, R. P. V. (2005). Surface-enhanced Raman spectroscopy. Analytical Chemistry, 77(17), 338-A.
[10] Zhang, X., Young, M. A., Lyandres, O., Van Duyne, R. P. (2005). Rapid detection of an anthrax biomarker by surface-enhanced Raman spectroscopy. Journal of the American Chemical Society, 127(12), 4484-4489.
[11] Zhang, X., Xiao, K., Dong, C., Wu, J., Li, X., Huang, Y. (2011). In situ Raman spectroscopy study of corrosion products on the surface of carbon steel in solution containing Cl− and. Engineering Failure Analysis, 18(8), 1981-1989.
[12] Ferraro, J. R. (2003). Introductory raman spectroscopy. Academic press.
[13] Driscoll, A. J., Harpster, M. H., Johnson, P. A. (2013). The development of surface-enhanced Raman scattering as a detection modality for portable in vitro diagnostics: progress and challenges. Physical Chemistry Chemical Physics, 15(47), 20415-20433.
[14] Sharma, B., Frontiera, R. R., Henry, A. I., Ringe, E., Van Duyne, R. P. (2012). SERS: materials, applications, and the future. Materials today, 15(1), 16-25.
[15] Schatz, G. C. (2001). Electrodynamics of nonspherical noble metal nanoparticles and nanoparticle aggregates. Journal of Molecular Structure: THEOCHEM, 573(1), 73-80.
[16] Zeisel, D., Deckert, V., Zenobi, R., Vo-Dinh, T. (1998). Near-field surface-enhanced Raman spectroscopy of dye molecules adsorbed on silver island films. chemical Physics letters, 283(5), 381-385.
[17] Li, W. H., Li, X. Y., Yu, N. T. (1999). Surface-enhanced resonance hyper-Raman scattering and surface-enhanced resonance Raman scattering of dyes adsorbed on silver electrode and silver colloid: a comparison study. Chemical physics letters, 312(1), 28-36.
[18] Cialla, D., März, A., Böhme, R., Theil, F., Weber, K., Schmitt, M., Popp, J. (2012). Surface-enhanced Raman spectroscopy (SERS): progress and trends. Analytical and bioanalytical chemistry, 403(1), 27-54.
[19] Li, J. F., Huang, Y. F., Ding, Y., Yang, Z. L., Li, S. B., Zhou, X. S., Wang, Z. L. (2010). Shell-isolated nanoparticle-enhanced Raman spectroscopy. nature, 464(7287), 392-395.
[20] Betz, J. F., Wei, W. Y., Cheng, Y., White, I. M.,Rubloff, G. W. (2014). Simple SERS substrates: powerful, portable, and full of potential. Physical Chemistry Chemical Physics, 16(6), 2224-2239.
[21] Love, S. A., Marquis, B. J., Haynes, C. L. (2008). Recent advances in nanomaterial plasmonics: fundamental studies and applications. Appl Spectrosc, 62(12), 346A-362A.
[22] Lin, X. M., Cui, Y., Xu, Y. H., Ren, B., Tian, Z. Q. (2009). Surface-enhanced Raman spectroscopy: substrate-related issues. Analytical and bioanalytical chemistry, 394(7), 1729-1745.
[23] Brown, R. J., Milton, M. J. (2008). Nanostructures and nanostructured substrates for surface—enhanced Raman scattering (SERS). Journal of Raman Spectroscopy, 39(10), 1313-1326.
[24] Banholzer, M. J., Millstone, J. E., Qin, L., Mirkin, C. A. (2008). Rationally designed nanostructures for surface-enhanced Raman spectroscopy. Chemical Society Reviews, 37(5), 885-897.
[25] Halvorson, R. A., Vikesland, P. J. (2010). Surface-enhanced Raman spectroscopy (SERS) for environmental analyses. Environmental science & technology, 44(20), 7749-7755.
[26] Gruenke, N. L., Cardinal, M. F., McAnally, M. O., Frontiera, R. R., Schatz, G. C.,Van Duyne, R. P. (2016). Ultrafast and nonlinear surface-enhanced Raman spectroscopy. Chemical Society Reviews, 45(8), 2263-2290.
[27] Sciau, P. (2012). Nanoparticles in Ancient Materials: The Metallic Lustre Decorations of Medieval Ceramics (Vol. 115, pp. 525-540). INTECH Open Access Publisher.
[28] Kneipp, K., Kneipp, H., Seifert, F. (1995). Near-infrared excitation profile study of surface-enhanced hyper-Raman scattering and

surface-enhanced Raman scattering by means of tunable mode-locked Ti: sapphire laser excitation. Chemical physics letters, 233(5), 519-524.

[29] Ko, H., Singamaneni, S., Tsukruk, V. V. (2008). Nanostructured surfaces and assemblies as SERS media. Small, 4(10), 1576-1599.

[30] Jain, P. K., Huang, X., El-Sayed, I. H., El-Sayed, M. A. (2008). Noble metals on the nanoscale: optical and photothermal properties and some applications in imaging, sensing, biology, and medicine. Accounts of chemical research, 41(12), 1578-1586.

[31] Freestone, I., Meeks, N., Sax, M., Higgitt, C. (2007). The Lycurgus cup—a roman nanotechnology. Gold Bulletin, 40(4), 270-277.

[32] Kneipp, K., Wang, Y., Kneipp, H., Perelman, L. T., Itzkan, I., Dasari, R. R., Feld, M. S. (1997). Single molecule detection using surface-enhanced Raman scattering (SERS). Physical review letters, 78(9), 1667.

[33] Li, W. H., Li, X. Y., Yu, N. T. (2000). Surface-enhanced hyper-Raman scattering and surface-enhanced Raman scattering studies of electroreduction of phenazine on silver electrode. Chemical Physics Letters, 327(3), 153-161.

[34] Milojevich, C. B., Mandrell, B. K., Turley, H. K., Iberi, V., Best, M. D., Camden, J. P. (2013). Surface-enhanced hyper-Raman scattering from single molecules. The Journal of Physical Chemistry Letters, 4(20), 3420-3423.

[35] Turley, H. K., Camden, J. P. (2014). A nonlinear approach to surface-enhanced sensing in the short-wave infrared. Chemical Communications, 50(12), 1472-1474.

[36] Gibson, K. F., Kazarian, S. G. Tip - enhanced Raman Spectroscopy.Encyclopedia of Analytical Chemistry.

[37] Yeo, B. S., Stadler, J., Schmid, T., Zenobi, R., Zhang, W. (2009). Tip-enhanced Raman Spectroscopy–Its status, challenges and future directions.Chemical Physics Letters, 472(1), 1-13.

[38] Pettinger, B. (2010). Single-molecule surface-and tip-enhanced Raman spectroscopy. Molecular Physics, 108(16), 2039-2059.

[39] Stöckle, R. M., Suh, Y. D., Deckert, V., Zenobi, R. (2000). Nanoscale chemical analysis by tip-enhanced Raman spectroscopy. Chemical Physics Letters, 318(1), 131-136.

[40] Bailo, E., & Deckert, V. (2008). Tip-enhanced Raman scattering. Chemical Society Reviews, 37(5), 921-930.

[41] Hayazawa, N., Saito, Y., Kawata, S. (2004). Detection and characterization of longitudinal field for tip-enhanced Raman spectroscopy. Applied Physics Letters, 85(25), 6239-6241.

[42] Kalinin, S. V., Gruverman, A. (2007). Scanning probe microscopy: electrical and electromechanical phenomena at the nanoscale (Vol. 1). Springer Science & Business Media.

[43] Hayazawa, N., Tarun, A., Taguchi, A., Furusawa, K. (2012). Tip-enhanced Raman spectroscopy. In Raman Spectroscopy for Nanomaterials Characterization (pp. 445-476). Springer Berlin Heidelberg.

[44] Yeo, B. S., Amstad, E., Schmid, T., Stadler, J., Zenobi, R. (2009). Nanoscale Probing of a Polymer - Blend Thin Film with Tip - Enhanced Raman Spectroscopy. Small, 5(8), 952-960.

[45] Jiang, N., Foley, E. T., Klingsporn, J. M., Sonntag, M. D., Valley, N. A., Dieringer, J. A., Van Duyne, R. P. (2012). Observation of multiple vibrational modes in ultrahigh vacuum tip-enhanced Raman spectroscopy combined with molecular-resolution scanning tunneling microscopy. Nano letters, 12(10), 5061-5067.

[46] Saito, Y., Verma, P., Masui, K., Inouye, Y., Kawata, S. (2009). Nano-scale analysis of graphene layers by tip-enhanced near-field Raman spectroscopy.Journal of Raman Spectroscopy, 40(10), 1434-1440.

[47] Synge, E. (1928). XXXVIII. A suggested method for extending microscopic resolution into the ultra-microscopic region. The London, Edinburgh, and Dublin Philosophical Magazine and Journal of Science, 6(35), 356-362.

[48] Wessel, J. (1985). Surface-enhanced optical microscopy. JOSA B, 2(9), 1538-1541.

[49] Anderson, M. S. (2000). Locally enhanced Raman spectroscopy with an atomic force microscope. Applied Physics Letters, 76(21), 3130-3132.

[50] Hayazawa, N., Inouye, Y., Sekkat, Z., Kawata, S. (2000). Metallized tip amplification of near-field Raman scattering. Optics Communications, 183(1), 333-336.

[51] Yeo, B. S., Zhang, W., Vannier, C., Zenobi, R. (2006). Enhancement of Raman signals with silver-coated tips. Applied spectroscopy, 60(10), 1142-1147.

[52] Hartschuh, A., Sánchez, E. J., Xie, X. S., Novotny, L. (2003). High-resolution near-field Raman microscopy of single-walled carbon nanotubes.Physical Review Letters, 90(9), 095503.

[53] Okuno, Y., Saito, Y., Kawata, S., Verma, P. (2013). Tip-enhanced Raman investigation of extremely localized semiconductor-to-metal transition of a carbon nanotube. Physical review letters, 111(21), 216101.

[54] Su, W., Roy, D. (2013). Visualizing graphene edges using tip-enhanced Raman spectroscopy. Journal of Vacuum Science & Technology B, 31(4), 041808.

[55] Kumar, N., Mignuzzi, S., Su, W., Roy, D. (2015). Tip-enhanced Raman spectroscopy: principles and applications. EPJ Techniques and Instrumentation, 2(1), 1-23.

[56] Bailo, E., Deckert, V. (2008). Tip- Enhanced Raman Spectroscopy of Single RNA Strands: Towards a Novel Direct- Sequencing Method. Angewandte Chemie International Edition, 47(9), 1658-1661.

[57] Neugebauer, U., Schmid, U., Baumann, K., Ziebuhr, W., Kozitskaya, S., Deckert, V., Popp, J. (2007). Towards a detailed understanding of bacterial metabolism—spectroscopic characterization of Staphylococcus epidermidis. ChemPhysChem, 8(1), 124-137.

[58] Barrios, C. A., Malkovskiy, A. V., Kisliuk, A. M., Sokolov, A. P., Foster, M. D. (2009). Highly stable, protected plasmonic nanostructures for tip enhanced Raman spectroscopy. The Journal of Physical Chemistry C, 113(19), 8158-8161.

[59] You, Y., Purnawirman, N. A., Hu, H., Kasim, J., Yang, H., Du, C., Shen, Z. (2010). Tip- enhanced Raman spectroscopy using single-crystalline Ag nanowire as tip. Journal of Raman Spectroscopy, 41(10), 1156-1162.

[60] Steidtner, J., Pettinger, B. (2007). High-resolution microscope for tip-enhanced optical processes in ultrahigh vacuum. Review of Scientific Instruments, 78(10), 103104.

[61] Zumbusch, A., Holtom, G. R., Xie, X. S. (1999). Three-dimensional vibrational imaging by coherent anti-Stokes Raman scattering. Physical review letters, 82(20), 4142.

[62] Cheng, J. X., Jia, Y. K., Zheng, G., Xie, X. S. (2002). Laser-scanning coherent anti-Stokes Raman scattering microscopy and applications to cell biology. Biophysical journal, 83(1), 502-509.

[63] Heinrich, C., Bernet, S., Ritsch-Marte, M. (2004). Wide-field coherent anti-Stokes Raman scattering microscopy. Applied physics letters, 84(5), 816-818.

[64] Day, J. P., Domke, K. F., Rago, G., Kano, H., Hamaguchi, H. O., Vartiainen, E. M., Bonn, M. (2011). Quantitative coherent anti-Stokes Raman scattering (CARS) microscopy. The Journal of Physical Chemistry B, 115(24), 7713-7725.

[65] Ganikhanov, F., Carrasco, S., Xie, X. S., Katz, M., Seitz, W., Kopf, D. (2006). Broadly tunable dual-wavelength light source for coherent anti-Stokes Raman scattering microscopy. Optics letters, 31(9), 1292-1294.

[66] Cheng, J. X., Xie, X. S. (2004). Coherent anti-Stokes Raman scattering microscopy: instrumentation, theory, and applications. The Journal of Physical Chemistry B, 108(3), 827-840.

[67] El-Diasty, F. (2011). Coherent anti-Stokes Raman scattering: spectroscopy and microscopy. Vibrational Spectroscopy, 55(1), 1-37.

[68] Lee, Y. J., & Cicerone, M. T. (2009). Single-shot interferometric approach to background free broadband coherent anti-Stokes Raman scattering spectroscopy*. Optics express, 17(1), 123-135.

[69] Ganikhanov, F., Evans, C. L., Saar, B. G., Xie, X. S. (2006). High-sensitivity vibrational imaging with frequency modulation coherent anti-Stokes Raman scattering (FM CARS) microscopy. Optics letters, 31(12), 1872-1874.

[70] Kiefer, W. (2008). Recent advances in linear and nonlinear Raman spectroscopy II. Journal of Raman Spectroscopy, 39(12), 1710-1725.

[71] Zimmerley, M., Lin, C. Y., Oertel, D. C., Marsh, J. M., Ward, J. L., Potma, E. O. (2009). Quantitative detection of chemical compounds in human hair with coherent anti-Stokes Raman scattering microscopy. Journal of biomedical optics, 14(4), 044019-044019.

[72] Chan, J. W., Winhold, H., Lane, S. M., Huser, T. (2005). Optical trapping and coherent anti-Stokes Raman scattering (CARS) spectroscopy of submicron-size particles. Selected Topics in Quantum Electronics, IEEE Journal of, 11(4), 858-863.

[73] Djaker, N., Lenne, P. F., Marguet, D., Colonna, A., Hadjur, C., Rigneault, H. (2007). Coherent anti-Stokes Raman scattering microscopy (CARS): Instrumentation and applications. Nuclear Instruments and Methods in Physics Research Section A: Accelerators, Spectrometers, Detectors and Associated Equipment, 571(1), 177-181.

[74] Evans, C. L., & Xie, X. S. (2008). Coherent anti-Stokes Raman scattering microscopy: chemical imaging for biology and medicine. Annu. Rev. Anal. Chem., 1, 883-909.
[75] Schie, I. W., Krafft, C., Popp, J. (2015). Applications of coherent Raman scattering microscopies to clinical and biological studies. Analyst, 140(12), 3897-3909.
[76] Hellerer, T., Axäng, C., Brackmann, C., Hillertz, P., Pilon, M., Enejder, A. (2007). Monitoring of lipid storage in Caenorhabditis elegans using coherent anti-Stokes Raman scattering (CARS) microscopy. Proceedings of the National Academy of Sciences, 104(37), 14658-14663.
[77] Müller, M., & Zumbusch, A. (2007). Coherent anti- Stokes Raman Scattering Microscopy. ChemPhysChem, 8(15), 2156-2170.
[78] Kox, M. H., Domke, K. F., Day, J. P., Rago, G., Stavitski, E., Bonn, M., Weckhuysen, B. M. (2009). Label- Free Chemical Imaging of Catalytic Solids by Coherent Anti- Stokes Raman Scattering and Synchrotron - Based Infrared Microscopy. Angewandte Chemie International Edition, 48(47), 8990-8994.
[79] Schafer, D., Squier, J. A., Maarseveen, J. V., Bonn, D., Bonn, M., Müller, M. (2008). In situ quantitative measurement of concentration profiles in a microreactor with submicron resolution using multiplex CARS microscopy.Journal of the American Chemical Society, 130(35), 11592-11593.
[80] Basiev, T. T., Sobol, A. A., Zverev, P. G., Ivleva, L. I., Osiko, V. V., Powell, R. C. (1999). Raman spectroscopy of crystals for stimulated Raman scattering. Optical materials, 11(4), 307-314.
[81] Woodbury, E. J., Ng, W. K. (1962). Ruby laser operation in near IR.Proceedings of the Institute of Radio Engineers, 50(11), 2367.
[82] White, J. C. (1987). Stimulated raman scattering. In Tunable lasers (pp. 115-207). Springer Berlin Heidelberg.
[83] Nandakumar, P., Kovalev, A., Volkmer, A. (2009). Vibrational imaging based on stimulated Raman scattering microscopy. New Journal of Physics, 11(3), 033026.
[84] Tipping, W. J., Lee, M., Serrels, A., Brunton, V. G., Hulme, A. N. (2016). Stimulated Raman scattering microscopy: an emerging tool for drug discovery. Chemical Society Reviews, 45(8), 2075-2089.
[85] Zhang, D., Wang, P., Slipchenko, M. N., Cheng, J. X. (2014). Fast vibrational imaging of single cells and tissues by stimulated Raman scattering microscopy. Accounts of chemical research, 47(8), 2282-2290.
[86] Freudiger, C. W., Min, W., Saar, B. G., Lu, S., Holtom, G. R., He, C., Xie, X. S. (2008). Label-free biomedical imaging with high sensitivity by stimulated Raman scattering microscopy. Science, 322(5909), 1857-1861.
[87] Kukura, P., Yoon, S., Mathies, R. A. (2006). Femtosecond stimulated Raman spectroscopy. Analytical chemistry, 78(17), 5952-5959.
[88] Boudon, V., Bermejo, D., Martínez, R. Z. (2013). High- resolution stimulated Raman spectroscopy and analysis of the ν 1, 2ν 1– ν 1, ν 2, 2ν 2, and 3ν 2– ν 2 bands of CF4. Journal of Raman Spectroscopy, 44(5), 731-738.
[89] Fu, D., Yu, Y., Folick, A., Currie, E., Farese Jr, R. V., Tsai, T. H., Wang, M. C. (2014). In vivo metabolic fingerprinting of neutral lipids with hyperspectral stimulated Raman scattering microscopy. Journal of the American Chemical Society, 136(24), 8820-8828.
[90] Mansfield, J. C., Littlejohn, G. R., Seymour, M. P., Lind, R. J., Perfect, S., Moger, J. (2013). Label-free chemically specific imaging in planta with stimulated Raman scattering microscopy. Analytical chemistry, 85(10), 5055-5063.
[91] Ploetz, E., Laimgruber, S., Berner, S., Zinth, W., Gilch, P. (2007). Femtosecond stimulated Raman microscopy. Applied Physics B, 87(3), 389-393.
[92] Nafie, L. A. (2014). Recent advances in linear and nonlinear Raman spectroscopy. Part VIII. Journal of Raman Spectroscopy, 45(11-12), 1326-1346.
[93] Smith, E., Dent, G. (2005). Introduction, basic theory and principles. Modern Raman spectroscopy-A practical approach, 1-21.
[94] Li, C. (2003). Identifying the isolated transition metal ions/oxides in molecular sieves and on oxide supports by UV resonance Raman spectroscopy. Journal of Catalysis, 216(1), 203-212.
[95] Wood, B. R., Caspers, P., Puppels, G. J., Pandiancherri, S., McNaughton, D. (2007). Resonance Raman spectroscopy of red blood cells using near-infrared laser excitation. Analytical and bioanalytical chemistry, 387(5), 1691-1703.
[96] Strommen, D. P., Nakamoto, K. (1977). Resonance Raman spectroscopy. Journal of Chemical Education, 54(8), 474.
[97] Marcus, M. A., Lewis, A. (1977). Kinetic resonance Raman spectroscopy: dynamics of deprotonation of the Schiff base of bacteriorhodopsin. Science, 195(4284), 1328-1330.
[98] http://forum.sci.ccny.cuny.edu/core_facilities/microscopy-imaging/raman-confocal/Confocal-raman-note.pdf
[99] Everall, N. (2004). Depth profiling with confocal Raman microscopy, part I. SPECTROSCOPY-SPRINGFIELD THEN EUGENE THEN DULUTH-, 19, 22-33.
[100] Gierlinger, N., Schwanninger, M. (2006). Chemical imaging of poplar wood cell walls by confocal Raman microscopy. Plant Physiology, 140(4), 1246-1254.
[101] Donev, E. U., Lopez, R., Feldman, L. C., Haglund Jr, R. F. (2009). Confocal Raman Microscopy across the Metal− Insulator Transition of Single Vanadium Dioxide Nanoparticles. Nano letters, 9(2), 702-706.
[102] Glenn, J. V., Beattie, J. R., Barrett, L., Frizzell, N., Thorpe, S. R., Boulton, M. E., Stitt, A. W. (2007). Confocal Raman microscopy can quantify advanced glycation end product (AGE) modifications in Bruch's membrane leading to accurate, nondestructive prediction of ocular aging. The FASEB journal, 21(13), 3542-3552.
[103] Etienne, M., Dossot, M., Grausem, J., Herzog, G. (2014). Combined Raman Microspectrometer and Shearforce Regulated SECM for Corrosion and Self-Healing Analysis. Analytical chemistry, 86(22), 11203-11210.
[104] Puppels, G. J., Schut, T. B., Sijtsema, N. M., Grond, M., Maraboeuf, F., De Grauw, C. G., Greve, J. (1995). Development and application of Raman microspectroscopic and Raman imaging techniques for cell biological studies. Journal of Molecular Structure, 347, 477-483.
[105] http://www.horiba.com/scientific/products/raman-spectroscopy/raman-imaging/]
[106] Schlücker, S., Schaeberle, M. D., Huffman, S. W., Levin, I. W. (2003). Raman microspectroscopy: a comparison of point, line, and wide-field imaging methodologies. Analytical Chemistry, 75(16), 4312-4318.
[107] Huang, Z., Teh, S. K., Zheng, W., Mo, J., Lin, K., Shao, X., Yeoh, K. G. (2009). Integrated Raman spectroscopy and trimodal wide-field imaging techniques for real-time in vivo tissue Raman measurements at endoscopy. Optics letters, 34(6), 758-760.
[108] Ling, J., Weitman, S. D., Miller, M. A., Moore, R. V., Bovik, A. C. (2002). Direct Raman imaging techniques for study of the subcellular distribution of a drug. Applied optics, 41(28), 6006-6017.
[109] Liu, Z., Li, X., Tabakman, S. M., Jiang, K., Fan, S., Dai, H. (2008). Multiplexed multicolor Raman imaging of live cells with isotopically modified single walled carbon nanotubes. Journal of the American Chemical Society, 130(41), 13540-13541.
[110] Gierlinger, N., Schwanninger, M. (2007). The potential of Raman microscopy and Raman imaging in plant research. Spectroscopy, 21(2), 69-89.
[111] Wartewig, S., Neubert, R. H. (2005). Pharmaceutical applications of Mid-IR and Raman spectroscopy. Advanced drug delivery reviews, 57(8), 1144-1170.
[112] Smith, G. D., Clark, R. J. (2004). Raman microscopy in archaeological science. Journal of Archaeological Science, 31(8), 1137-1160.
[113] Maaß, P., Peißker, P. (Eds.). (2011). Handbook of hot-dip galvanization. John Wiley & Sons.
[114] Hackerman, N. (1987). The theory and practice of corrosion and its control in industry. Langmuir, 3(6), 922-924.
[115] Perez, T. E. (2013). Corrosion in the Oil and Gas Industry: An Increasing Challenge for Materials. JOM, 65(8), 1033-1042.
[116] Kermani, M. B., Morshed, A. (2003). Carbon dioxide corrosion in oil and gas production-A compendium. Corrosion, 59(8), 659-683.
[117] Roberge, P. R. (2007). Corrosion inspection and monitoring (Vol. 2). John Wiley & Sons.
[118] http://www.npl.co.uk/science-technology/advanced-materials/national-corrosion-service/ , slides]
[119] Gangloff, R. P., Shipilov, S. A., Jones, R. H., Olive, J. M., Rebak, R. B. (2008). Environment-induced cracking of materials. Crit. issues hydrog. assist. crack. stuctural alloy. Oxford, UK: Elsevier, 14.
[120] Choi, H., Tonsuwannarat, T. (2002, January). Unique Roles of Hydrocarbons in Flow-Induced Sweet Corrosion of X-52 Carbon Steel in Wet Gas Condensate Producing Wells. In CORROSION 2002. NACE International.
[121] Nyborg, R. (2002, January). Overview of CO2 corrosion models for wells and pipelines. In CORROSION 2002. NACE International.
[122] Makar, J., Chagnon, N. (1999). Inspecting systems for leaks, pits, and corrosion. American Water Works Association. Journal, 91(7), 36.

[123]Safizadeh, M. S., Azizzadeh, T. (2012). Corrosion detection of internal pipeline using NDT optical inspection system. NDT & E International, 52, 144-148.

[124]Ghods, P., Isgor, O. B., Bensebaa, F., Kingston, D. (2012). Angle-resolved XPS study of carbon steel passivity and chloride-induced depassivation in simulated concrete pore solution. Corrosion Science, 58, 159-167.

[125]Fajardo, S., Bastidas, D. M., Ryan, M. P., Criado, M., McPhail, D. S., Bastidas, J. M. (2010). Low-nickel stainless steel passive film in simulated concrete pore solution: A SIMS study. Applied surface science, 256(21), 6139-6143.

[126]Souier, T., Martin, F., Bataillon, C., Cousty, J. (2010). Local electrical characteristics of passive films formed on stainless steel surfaces by current sensing atomic force microscopy. Applied Surface Science, 256(8), 2434-2439.

[127]Criado, M., Martínez‐Ramirez, S., Fajardo, S., Gómez, P. P., Bastidas, J. M. (2013). Corrosion rate and corrosion product characterisation using Raman spectroscopy for steel embedded in chloride polluted fly ash mortar. Materials and Corrosion, 64(5), 372-380.

[128]Hazan, E., Sadia, Y., Gelbstein, Y. (2013). Characterization of AISI 4340 corrosion products using Raman spectroscopy. corrosion Science, 74, 414-418.

[129]Fabis, P., Brown, C., Rockett, T., Heidersbach, R. (1981). An Infrared and Raman spectroscopy study of the corrosion products on carbon steel and weathering steel. Oxidation of Metals, 16(5-6), 399-407.

[130]Criado, M., Martínez-Ramirez, S., Bastidas, J. M. (2015). A Raman spectroscopy study of steel corrosion products in activated fly ash mortar containing chlorides. Construction and Building Materials, 96, 383-390.

[131]Cook, D. C. (2005). Spectroscopic identification of protective and non-protective corrosion coatings on steel structures in marine environments. Corrosion Science, 47(10), 2550-2570.

[132]Neff, D., Bellot‐Gurlet, L., Dillmann, P., Reguer, S., Legrand, L. (2006). Raman imaging of ancient rust scales on archaeological iron artefacts for long‐term atmospheric corrosion mechanisms study. Journal of Raman spectroscopy, 37(10), 1228-1237.

[133]Antony, H., Maréchal, L., Legrand, L., Chaussé, A., Perrin, S., Dillmann, P. (2004). Electrochemical study of lepidocrocite reduction and redox cycling for the mechanistic modelling of atmospheric corrosion. In Eurocorr Conference, Paper (Vol. 277).

[134]Yamashita, M., Miyuki, H., Matsuda, Y., Nagano, H., Misawa, T. (1994). The long term growth of the protective rust layer formed on weathering steel by atmospheric corrosion during a quarter of a century. Corrosion Science, 36(2), 283-299.

[135]Dillmann, P., Mazaudier, F., Hoerle, S. (2004). Advances in understanding atmospheric corrosion of iron. I. Rust characterisation of ancient ferrous artefacts exposed to indoor atmospheric corrosion. Corrosion Science, 46(6), 1401-1429.

[136]Bellot-Gurlet, L., Neff, D., Reguer, S., Monnier, J., Saheb, M., Dillmann, P. (2009, September). Raman studies of corrosion layers formed on archaeological irons in various media. In Journal of Nano Research (Vol. 8, pp. 147-156). Trans Tech Publications.

[137]Savoye, S., Legrand, L., Sagon, G., Lecomte, S., Chausse, A., Messina, R., Toulhoat, P. (2001). Experimental investigations on iron corrosion products formed in bicarbonate/carbonate-containing solutions at 90 C. Corrosion Science, 43(11), 2049-2064.

[138]Nie, X., Li, X., Du, C., Huang, Y., Du, H. (2009). Characterization of corrosion products formed on the surface of carbon steel by Raman spectroscopy. Journal of Raman Spectroscopy, 40(1), 76-79.

[139]Ohtsuka, T., Tanaka, S. (2015). Monitoring the development of rust layers on weathering steel using in situ Raman spectroscopy under wet-and-dry cyclic conditions. Journal of Solid State Electrochemistry, 19(12), 3559-3566.

[140]Reguer, S., Neff, D., Bellot‐Gurlet, L., Dillmann, P. (2007). Deterioration of iron archaeological artefacts: micro‐Raman investigation on Cl‐containing corrosion products. Journal of Raman Spectroscopy, 38(4), 389-397.

[141]Neff, D., Reguer, S., Bellot‐Gurlet, L., Dillmann, P., Bertholon, R. (2004). Structural characterization of corrosion products on archaeological iron: an integrated analytical approach to establish corrosion forms. Journal of Raman Spectroscopy, 35(8‐9), 739-745.

[142]Saheb, M., Neff, D., Dillmann, P., Matthiesen, H., Foy, E. (2008). Long-term corrosion behaviour of low-carbon steel in anoxic environment: characterisation of archaeological artefacts. Journal of Nuclear Materials,379(1), 118-123.

[143]Reguer, S., Neff, D., Bellot‐Gurlet, L., Dillmann, P. (2007). Deterioration of iron archaeological artefacts: micro‐Raman investigation on Cl‐containing corrosion products. Journal of Raman Spectroscopy, 38(4), 389-397.

[144]Monnier, J., Bellot‐Gurlet, L., Baron, D., Neff, D., Guillot, I., Dillmann, P. (2011). A methodology for Raman structural quantification imaging and its application to iron indoor atmospheric corrosion products. Journal of Raman Spectroscopy, 42(4), 773-781.

[145]De Faria, D. L. A., Venâncio Silva, S., De Oliveira, M. T. (1997). Raman microspectroscopy of some iron oxides and oxyhydroxides. Journal of Raman spectroscopy, 28(11), 873-878.

[146]El Mendili, Y., Bardeau, J. F., Randrianantoandro, N., Grasset, F., Greneche, J. M. (2012). Insights into the mechanism related to the phase transition from γ-Fe2O3 to α-Fe2O3 nanoparticles induced by thermal treatment and laser irradiation. The Journal of Physical Chemistry C, 116(44), 23785-23792.

[147]Singh, J. K., Singh, D. D. N. (2012). The nature of rusts and corrosion characteristics of low alloy and plain carbon steels in three kinds of concrete pore solution with salinity and different pH. Corrosion Science, 56, 129-142.

[148]Colomban, P., Cherifi, S., Despert, G. (2008). Raman identification of corrosion products on automotive galvanized steel sheets. Journal of Raman Spectroscopy, 39(7), 881-886.

[149]Dubois, F., Mendibide, C., Pagnier, T., Perrard, F., Duret, C. (2008). Raman mapping of corrosion products formed onto spring steels during salt spray experiments. A correlation between the scale composition and the corrosion resistance. Corrosion Science, 50(12), 3401-3409.

[150]Balasubramaniam, R., Kumar, A. R., Dillmann, P. (2003). Characterization of rust on ancient Indian iron. Current Science, 85(11), 1546-1555.

[151]Antunesa, R. A., Costaa, I., de Fariab, D. L. A. (2003). Characterization of Corrosion Products Formed on Steels in The First Months of Atmospheric Exposure. Matéria, 8(1), 27-34.

[152]Guzonas, D. A., Rochefort, P. A., Turner, C. W. (1998). Corrosion Product Characterisation by Fibre Optic Raman Spectroscopy. Canadian Nuclear Society Societe Nucleaire Canadienne, 628.

[153]Eckold, P., Rolff, M., Niewa, R., Hügel, W. (2015). Synthesis, characterization and in situ Raman detection of Sn 3 O 2 (OH) 2− x Cl x phases as intermediates in tin corrosion. Corrosion Science, 98, 399-405.

[154]Stowe, A. C., Smyrl, N. (2012). Raman spectroscopy of lithium hydride corrosion: Selection of appropriate excitation wavelength to minimize fluorescence. Vibrational Spectroscopy, 60, 133-136.

[155]Puglieri, T. S., de Faria, D. L., Cavicchioli, A. (2014). Indoor corrosion of Pb: Effect of formaldehyde concentration and relative humidity investigated by Raman microscopy. Vibrational Spectroscopy, 71, 24-29.

[156]Maslar, J. E., Hurst, W. S., Bowers, W. J., Hendricks, J. H. (2001). In situ Raman spectroscopic investigation of zirconium–niobium alloy corrosion under hydrothermal conditions. Journal of nuclear materials, 298(3), 239-247.

[157]Amme, M., Renker, B., Schmid, B., Feth, M. P., Bertagnolli, H., Döbelin, W. (2002). Raman microspectrometric identification of corrosion products formed on UO 2 nuclear fuel during leaching experiments. Journal of nuclear materials, 306(2), 202-212.

[158]Frost, R. L. (2003). Raman spectroscopy of selected copper minerals of significance in corrosion. Spectrochimica Acta Part A: Molecular and Biomolecular Spectroscopy, 59(6), 1195-1204.

[159]Colomban, P. (2011). Potential and drawbacks of Raman (micro) spectrometry for the understanding of iron and steel corrosion. INTECH Open Access Publisher.

[160]Burgio, L., Clark, R. J. (2001). Library of FT-Raman spectra of pigments, minerals, pigment media and varnishes, and supplement to existing library of Raman spectra of pigments with visible excitation. Spectrochimica Acta Part A: Molecular and Biomolecular Spectroscopy, 57(7), 1491-1521.

[161]Bell, I. M., Clark, R. J., Gibbs, P. J. (1997). Raman spectroscopic library of natural and synthetic pigments (pre-≈ 1850 AD). Spectrochimica Acta Part A: Molecular and Biomolecular Spectroscopy, 53(12), 2159-2179.

[162]Bouchard, M., Smith, D. C. (2003). Catalogue of 45 reference Raman spectra of minerals concerning research in art history or archaeology,

especially on corroded metals and coloured glass. Spectrochimica Acta Part A: Molecular and Biomolecular Spectroscopy, 59(10), 2247-2266.

[163] Brody, R. H., Edwards, H. G., Pollard, A. M. (2002). Fourier transform - Raman spectroscopic study of natural resins of archaeological interest.Biopolymers, 67(2), 129-141.

[164] Vandenabeele, P., Edwards, H. G., Moens, L. (2007). A decade of Raman spectroscopy in art and archaeology. Chemical Reviews, 107(3), 675-686.

[165] http://www.horiba.com/fileadmin/uploads/Scientific/Documents/Raman/SO-TN02_- _Searching_spectral_databases_with_LabSpec_6.pdf

Dr Paul Rostron is professor of Chemistry and Corrosion at the Petroleum Institute, ADNOC's University and Research Center. He has taught courses, both undergraduate and post graduate in Chemistry and in Corrosion for more than 20 Years, as well as conducting masterclasses in corrosion globally. Current research topics include the synthesis of novel corrosion inhibitors, mitigation of biofouling, atmospheric corrosion mapping, and is building a flow – loop for corrosion in pipeline studies. Currently he is a member of the Board of Directors for NACE UAE section, and was recently chairman of the section as well as a member of the Institute of Corrosion and Chartered Chemist of the Royal Society of Chemistry.